Optics Communications 281 (2008) 4840–4843

Contents lists available at ScienceDirect

Optics Communications

journal homepage: www.elsevier.com/locate/optcom

Focal waveforms with tunable carrier frequency using dispersive aperturing

Carlos J. Zapata-Rodríguez

Department of Optics, University of Valencia, Dr. Moliner 50, E-46100 Burjassot, Spain

ARTICLE INFO

Article history:
Received 20 March 2008
Received in revised form 22 June 2008
Accepted 25 June 2008

PACS:
42.25.−p
41.85.−p

Keywords:
Wave optics
Beam optics

ABSTRACT

We introduce the concept of dispersive aperturing involving a beam truncation by hard-edge apertures where diameter of the processed beam changes upon frequency. Applied to focused waves, this procedure transforms power spectra at the focal point (and the surroundings). Waveforms at focus conserve pulse duration but carrier frequency may be altered substantially. In principle, some degrees of freedom allow carrier-frequency tuning at convenience.

1. Introduction

Focal waves have been the subject of intense investigation in past decades [1–4]. With the advent of commercial femtosecond lasers, broadband focused beams have attracted a great interest in recent years [5,6]. In the focal region, ultrafast wavefields demonstrate a behaviour that deviates of that observed for time-harmonic radiation [7,8]. Monochromatic constituents exhibit different spot sizes involving off-axis red shifts and spectral anomalies near phase singularities [9–11]. In the focal point, spectrum is factorized by a term $-\mathrm{i}\,k$, where $k=\omega/c$ denotes the wavenumber (c is phase velocity in vacuum), leading to the well-known time-derivative response [12,13].

The above-mentioned phenomena are attributed to nondispersive spatial filtering of broadband wavefields. Aperturing of spherical waves is performed in a way such that the pupil-induced beam diameter has a constant value. However, we may circumvent this restriction using glass lenses and, in general, image-forming elements with dispersive characteristics. Recently, we have exploited kinoform-type zone plates [14] to compensate chromatic mismatching of the point spread function (PSF) in the focal plane [15,16] and also along the optical axis [17]. The essential idea consists in imaging a hard-edge aperture with the help of highly-dispersive lenses, constructing a new limiting element with spectrally-tunable width. Numerical aperture of such focal waves may vary rapidly upon frequency and, thus, power spectra at focus are expected also to be altered significantly.

In this paper, we investigate in-focus spectral and temporal properties of pulsed fields under dispersive aperturing. The paper is organized as follows. In Section 2, the basic grounds on scalar, nonparaxial, focal wavefields with apertured spherical wavefronts are reviewed, giving emphasis to time-domain transformations induced by diffraction. In Section 3 an optical arrangement is reported in order to achieve dispersive aperturing. Anomalous dispersion is investigated in Section 4 providing red shifts and blue shifts but, in the meanwhile, maintaining the pulse duration of the inputs. Finally, in Section 5 the main conclusions are outlined.

2. On-axis diffraction-induced spectral shift

Let us consider a uniform plane wave of (amplitude) spectrum $S(\omega)$ collected by a infinity-tube nondispersive microscope objective. In this paper, we neglect pulse stretching induced by material dispersion of lenses. In the frequency domain, the focal field under the sine condition [18,19] is S times the PSF,

$$h(\mathbf{r})=-\mathrm{i}k\int_0^{\alpha}J_0(kr\sin\phi)\cos^{1/2}\phi\sin\phi\,\mathrm{d}\phi, \tag{1}$$

where $r=\|\mathbf{r}\|$, J_0 is the Bessel function of the first kind and order 0, and $\sin\alpha$ is the numerical aperture of the objective lens (in air). The focal wavefield is modelled within a scalar regime for simplicity, which restricts our analysis to low and moderate numerical apertures. In particular, PSF at the focal point reduces to

$$h(\mathbf{0})=\frac{-2\mathrm{i}k}{3}(1-\cos^{3/2}\alpha), \tag{2}$$

E-mail address: carlos.zapata@uv.es

0030-4018/$ - see front matter © 2008 Elsevier B.V. All rights reserved.
doi:10.1016/j.optcom.2008.06.065

which is proportional to the wavenumber. In the paraxial regime ($\sin\alpha \approx \alpha$) we have an analytical expression of the PSF giving

$$h_p(\mathbf{r}) = \frac{-\mathrm{i}\alpha J_1(kr\alpha)}{r}, \tag{3}$$

so that on-axis spectrum $h_p(\mathbf{0}) = -\mathrm{i}k\alpha^2/2$ is proportional to the squared numerical aperture.

Some consequences arise from the fact that on-axis spectrum differs from S by the factor $h(\mathbf{0})$, also called spectral modifier. If the numerical aperture is conserved for different frequencies, which is a common assumption for achromatic lens systems, the spectral modifier is proportional to the frequency and thus input spectrum is transformed into a focal spectrum $\propto -\mathrm{i}\omega S$. In the time domain, this sort of transformation refers on to a derivative of the waveform. In Fig. 1a we plot the normalized power spectrum at focus when (amplitude) inputs are of the Poisson type,

$$S(\omega) = S_0\left(\frac{\omega}{\omega_0}\right)^s \exp(-\tau\omega), \tag{4}$$

where S_0 and $\tau > 0$ are constant parameters, and $s = \omega_0\tau - 1$ in order to have a carrier (mean) envelope $\omega_0 = \bar{\omega}$ derived as

$$\bar{\omega}(S) = \frac{\int_0^\infty S(\omega)\omega \mathrm{d}\omega}{\int_0^\infty S(\omega)\mathrm{d}\omega}. \tag{5}$$

A blue shift $1/\tau$ is manifested at focus, computed from the difference of the mean frequency at focus $\bar{\omega}$ and ω_0. Along the pulse duration $2\Delta t$, where

$$\Delta t \approx \sqrt{\frac{\tau \log 2}{\omega_0}}, \tag{6}$$

however, the observed carrier frequency is unaltered (see Fig. 1). Moreover, the carrier–envelope phase is shifted by a quarter of a cycle.

Numerical aperture is determined by the photo-geometric characteristics of the microscope objective. However, we may modify (decrease) α by inserting a clear aperture of radius R in the mean path of the impinging plane wave in such a way that

$$\sin\alpha = \frac{R}{f_m}, \tag{7}$$

where f_m is the focal distance of the microscope objective. Assuming achromaticity of the lens system, hard-edge aperturing imposes that α remains unaltered at different frequencies. In this paper we consider using highly-dispersive lenses to alter chromatically the optical-limiting features of the clear aperture. As a consequence, we might derive an overall beam truncation diameter $2R$ varying upon angular frequency and thus $\alpha \equiv \alpha(\omega)$.

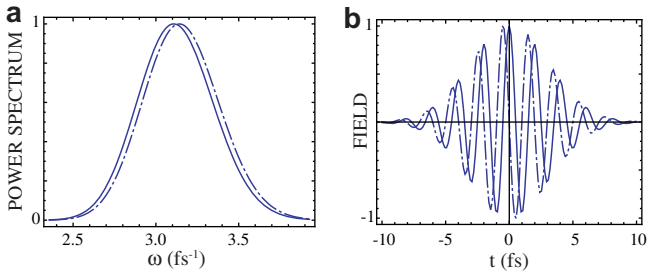

Fig. 1. Normalized (a) power spectrum and (b) waveform of input (solid curve) and focused (dashed-dotted curve) beams. Poisson spectrum is of carrier frequency $\omega_0 = 3.14\ \mathrm{fs}^{-1}$ and parameter $\tau = 30$ fs.

3. Dispersive control over aperturing

In Fig. 2 we represent an optical system capable of modifying chromatically the truncation diameter impinging onto the objective microscope. This setup follows the architecture of others reported elsewhere [15–17,20]. In the input plane, where we place a kinoform-type zone plate ZP_1 of dispersive focal distance $-Z\omega/\omega_0$, a plane wave of spectrum S enters into the system. Before considering beam aperturing, the pulsed beam is conveniently dispersed by passing through ZP_1 and the afocal doublet formed of achromatic lenses L_1 and L_2. In the figure, f denotes focal distance of each achromatic refractive lens. In the aperture plane (x,y), the illuminating system generates a wavefield

$$-SM\eta \exp\left[-\mathrm{i}\frac{k}{2f_a}(x^2+y^2)\right], \tag{8}$$

where

$$M = \frac{Z\omega}{Z\omega - a\omega_0}, \tag{9}$$

$$f_a = a - \frac{Z\omega}{\omega_0}, \tag{10}$$

the real amplitude $|\eta|$ stands for material absorption of lenses and efficiency of zone plates, and $\arg(\eta) = k\,L$, being L the optical path length of a light ray traversing the arrangement of lenses, along the optical axis, from the input plane to the aperture plane; from hereon we ignore this sort of cumulative terms considering $\eta = 1$. Also, a stands for the distance from the aperture plane to the back focal plane of L_2. The approach given in Eq. (8) is valid if f_a is sufficiently longer than the aperture radius within the spectral band $|S|$ takes significant values ($|\omega - \omega_0| < \sigma$). Equivalently, point F in Fig. 2 should be located sufficiently far from the aperture plane in a broadband around ω_0. Therefore, cases where a approaches to Z are excluded in this study.

After illuminating the clear aperture conveniently, the truncated pulse is incident upon a second zone plate ZP_2 of focal distance $Z\omega/\omega_0$. Irrespective from the frequency of every spectral constituent, the target of ZP_2 is to generate a plane wavefront of the dispersed pulse. Following a straightforward calculation, we may estimate the wavefield at a plane immediately behind ZP_2 as

$$\Phi(\mathbf{r}) = -ST\left(\frac{\mathbf{r}}{M}\right), \tag{11}$$

where $T(\mathbf{r})$ stands for the amplitude transmittance of the aperture. This geometric approach applies in the limit $k \to \infty$ but gives accurate results if the aperture diameter is significantly larger (by several orders of magnitude) than the wavelength $2\pi c/\omega_0$. Finally, note that the minus sign in Eqs. (8) and (11) represent the Guoy phase shift originated after focusing at F (see Fig. 2), changing the carrier–envelope phase of the pulsed beam.

From Eq. (11) we infer that if the field emerging from ZP_2 is a replica of the aperture transmittance magnified by the dispersive parameter $M(\omega)$, truncation (given by the radius R) of the wavefield impinging onto the microscope objective is also spectrally

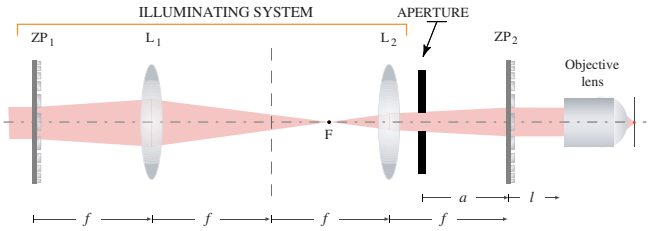

Fig. 2. Schematic depiction of the hybrid diffractive–refractive optical system.

dispersed. Specifically $R = R_0|M/M_0|$, where subindex 0 is referred to values at ω_0. Considering the sine condition (see Eq. (7)) we finally have

$$\sin\alpha(\omega) = \left|\frac{M}{M_0}\right| \sin\alpha_0. \tag{12}$$

We point out that an interval of values of the ratio a/Z may lead magnifications M such that Eq. (12) provides complex solutions for α. We clarify aspects of this question below.

Let us first investigate dispersive magnification at $\omega \approx \omega_0$. By means of a series expansion around ω_0 we may derive

$$\frac{M}{M_0} \approx 1 + \mu\frac{\omega - \omega_0}{\omega_0}, \tag{13}$$

where $\mu = a/(a - Z)$. In Fig. 3a we plot μ versus a/Z. If $0 < a < Z$ (or $Z < a < 0$ for negative ZP_2) μ is negative and therefore magnification decreases upon frequency. Consequently, proximity of clear aperture to ZP_2 provides numerical apertures following negative dispersion. Otherwise magnification shows positive dispersion. In Fig. 3b–d we plot absolute values of the relative magnification M/M_0. Moderate dispersion, both negative and positive, is shown in Fig. 3b and c. However, abrupt changes near ω_0 are found at a approaching to Z due to a singularity shown in figures at $\omega/\omega_0 = a/Z$.

In realistic circumstances, the microscope objective may also apply an additional aperturing. In the absence of the clear screen, the numerical aperture of the focused beam, determined by the objective lens pupils, is provided by $\sin\alpha_{ob}$. When the leading aperture is inserted, the hard-edge element dominating beam limiting determines the numerical aperture of the focal wavefield, computed as $\min[\sin\alpha(\omega), \sin\alpha_{ob}]$. Under such a consideration, complex solutions of α calculated from Eq. (12) are lacking interest. Moreover, we may speak of a dispersive regime if $\sin\alpha(\omega) < \sin\alpha_{ob}$ for the bandwidth $|\omega - \omega_0| < \sigma$, and a nondispersive regime if $\sin\alpha(\omega) > \sin\alpha_{ob}$. Broadband pulses may partially participate of both regimes. In this paper, obviously, we focus our attention mainly onto the dispersive regime.

4. Particular cases

The focusing optical system of Fig. 2 provides a wavefield at focus of the microscope objective given the product of the input spectrum and the spectral modifier of Eq. (2),

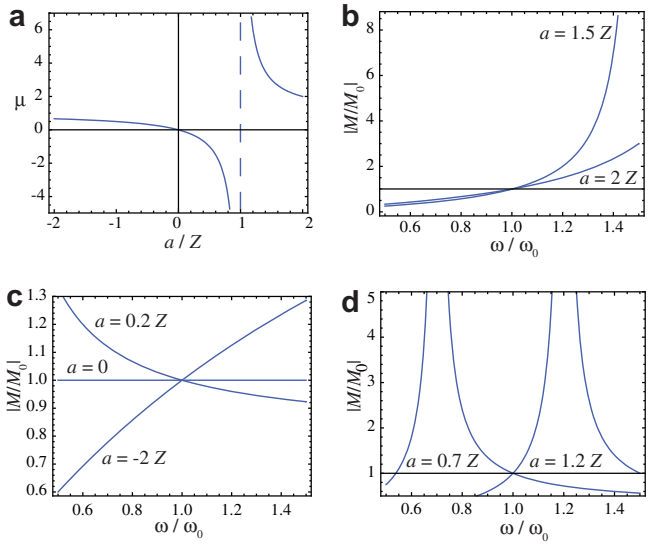

Fig. 3. (a) Plot of μ with respect to a/Z. (b–d) Study of M/M_0 for different values of a/Z.

$$S_f(\omega) = \frac{2ik(\omega)S(\omega)}{3}\left[1 - \cos^{3/2}\alpha(\omega)\right], \tag{14}$$

including the Guoy phase shift $\exp(i\pi)$. In the dispersive regime, numerical aperture is evaluated from Eq. (12) for different constituents of the spectrum S. Waveforms at focus are then computed using a one-dimensional Fourier transform,

$$s_f(t) = \Re\int_0^\infty S_f(\omega)\exp(-i\omega t)d\omega. \tag{15}$$

Here we assume S is function allowing a factorization of the form

$$s_f(t) = \sin(\omega_0 t)e(t), \tag{16}$$

where the envelope $e(t)$ varies slowly in comparison with the sine function. The carrier frequency ω_0 is computed from Eq. (5) as the mean frequency $\bar{\omega}(S_f)$. We point out that Poisson-type spectra are of this kind.

The carrier frequency for S commonly differs from that found for S_f due to the spectral modifier. Blue shifts and red shifts appears displacing the limiting aperture thus varying the axial distance a. Obviously, if $a = 0$, the hybrid diffractive–refractive optical system is unable to achieve a dispersive aperturing effect since $M = M_0$, keeping magnification invariant at different frequencies. Only the term $k(\omega)$ modifies spectrally the input S thus providing the aforementioned time-derivative effect over the focal waveform.

In Fig. 4 we represent carrier frequencies $\bar{\omega}(S_f)$ and spectral widths $\sigma(S_f)$ (standard deviation of ω with spectral distribution S_f) at different displacements of the dispersive pupil aperture. Complex i in Eq. (14) may be removed in the calculation in order to manage purely-real nonnegative magnitudes. In the numerical computation, again, spectrum S is of the Poisson type (normalization $S_0 = 1$ is used) with carrier frequency $\omega_0 = 3.14$ fs^{-1} and length $\tau = 30$ fs. When we increase $a/Z \gtrsim 0$, negative dispersion induces a red shift that might compensate the inherent blue shift arisen from the term k. Concretely at $a = Z/3$, power spectrum resembles that of the input pulse $|S|^2$ (a convenient normalization is required), with deviations lower than 0.9%. Consequently, diffraction-induced blue shifts are cancelled using dispersive aperturing. In the paraxial regime, incidentally, such a dispersive arrangement generates focal wavefields with achromatic response along the optical axis [17].

Equivalently, an achromatic effect in the transverse focal plane is attained if $a = Z/2$ (see also Ref. [16]). The Airy disk of the PSF in Eq. (3) conserves its width within a narrow band around the carrier frequency. This effect may be achieved since $k\alpha$ from the argument of J_1 has a stationary point at $\omega = \omega_0$ (see Refs. [16,20]); thus $k\alpha \approx k_0\alpha_0$. As a consequence, the spectral modifier follows a dependence ω^{-1}, inducing a time-antiderivative effect over the focal waveform, as shown in Fig. 5.

Extremal redshift is attained at $a/Z = 0.82$, obtaining $\bar{\omega} = 2.88$ fs^{-1}. From this aperture location up to $a/Z = 1.23$, where $\bar{\omega} = 3.49$ fs^{-1}, a strong spectral shift (from blue to red) may be

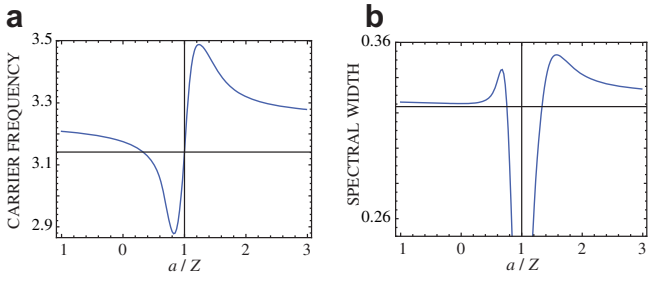

Fig. 4. (a) Carrier frequency $\bar{\omega}$ and (b) spectral width σ at focus for different values of the ratio a/Z. Units are in fs^{-1}. The origin of the y axis corresponds to magnitudes for input S.

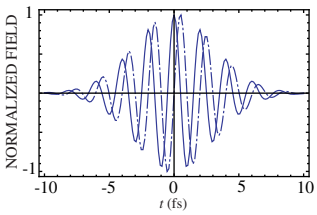

Fig. 5. Input waveform (solid line) and s_f at $a = Z/2$ (dashed-dotted line) demonstrating an anti-derivative response.

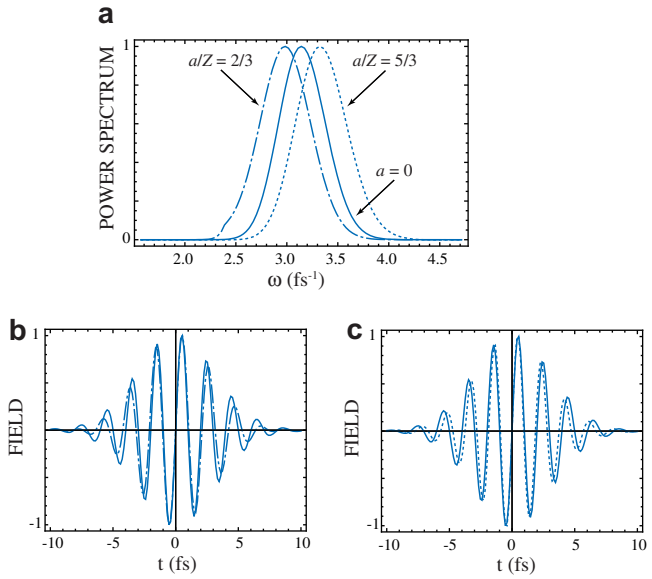

Fig. 6. Normalized (a) power spectrum and (b and c) waveform of focused beams. Solid curve corresponds to nondispersive aperturing, and dotted curve and dashed-dotted curve corresponds to different dispersive aperturings. Poisson spectrum is of carrier frequency $\omega_0 = 3.14\ \mathrm{fs}^{-1}$ and parameter $\tau = 30$ fs.

tuned. When a approaches to Z the illuminating system focuses F near the aperture in a band around ω_0. If the aperture is sufficiently small to neglect beam aperturing of diffractive–refractive lenses, transmittance varies sharply upon frequency so that the dispersive arrangement mainly performs a spectral filtering. Furthermore, beam aperturing at the exit plane is significantly weak. As a consequence, the microscope objective determines beam aperturing of the impinging quasimonochromatic (see Fig. 4b) wavefield, a situation that is out of our scope.

Significant blue shifts, however, may be achieved without loss of bandwidth at $a/Z \gtrapprox 1$. In Fig. 6a we compare normalized power spectra $|S_f|^2$ at focus placing the clear aperture at different positions within the dispersive regime. Enhancement of either lower or higher frequencies than input ω_0 attributed to dispersive aperturing is performed maintaining the spectral width of the input wavefield. Therefore, invariant pulse duration is observed at focus whereas carrier frequency is balanced at will (see Fig. 6b and c).

5. Conclusions

In this paper, dispersive aperturing is established as a tool for tuning spectra of focused waves. Modification of the beam diameter is spectrally distinctive using kinoform-type zone plates, which have a strong longitudinal chromatic aberration, as a first step before a microscope objective focuses light. Our proposal is simple but, obviously, not unique in order to achieve dispersive aperturing; alternative designs of optical arrangements employing highly-dispersive refractive lenses may be found (apart from aforementioned cites, see Ref. [21]) with similar spectral features. Here, the pupil aperture is then displaced conveniently to regulate the beam limiting and, subsequently, the numerical aperture of the focused wavefield at different frequencies.

Numerical simulations have been performed using Poisson-type spectra corresponding to few-cycles optical pulses. We have found conditions for carrier-frequency tuning at focus at the cost of bandwidth narrowing; however, such a spectral filtering is neglected in this manuscript. Considerable blue and red shifts may be accomplished in a wide range of aperture positions keeping unaltered bandwidths. Pulse reforms at predetermined carrier frequencies are thus achieved by simply dynamic aperturing.

Acknowledgement

This research was funded by the Generalitat Valenciana under the project GV/2007/043.

References

[1] E. Collet, E. Wolf, Opt. Lett. 5 (1980) 264.
[2] J.J. Stamnes, B. Spjelkavik, Opt. Commun. 40 (1981) 81.
[3] Y. Li, J. Opt. Soc. Am. A 4 (1987) 1349.
[4] C.J.R. Sheppard, M. Gu, J. Mod. Opt. 40 (1993) 1631.
[5] M. Kempe, U. Stamm, B. Wilhelmi, W. Rudolph, J. Opt. Soc. Am. B 9 (1992) 1158.
[6] M. Kempe, W. Rudolph, Phys. Rev. A 48 (1993) 4721.
[7] M.A. Porras, Phys. Rev. E 58 (1998) 1086.
[8] M.A. Porras, Phys. Rev. E 65 (2002) 026606.
[9] G. Gbur, T.D. Visser, E. Wolf, Phys. Rev. Lett. 88 (2002) 013901.
[10] C.J. Zapata-Rodríguez, J.A. Monsoriu, J. Opt. Soc. Am. A 21 (2004) 2418.
[11] C.J. Zapata-Rodríguez, Opt. Commun. 257 (2006) 9.
[12] A.E. Kaplan, J. Opt. Soc. Am. B 15 (1998) 951.
[13] C.J. Zapata-Rodríguez, Opt. Commun. 263 (2006) 131.
[14] V. Moreno, J.F. Román, J.R. Salgueiro, Am. J. Phys. 65 (1997) 556.
[15] C.J. Zapata-Rodríguez, J. Opt. Soc. Am. A 24 (2007) 675.
[16] C.J. Zapata-Rodríguez, M.T. Caballero, Opt. Express 15 (2007) 15308.
[17] C.J. Zapata-Rodríguez, P. Andrés, G. Mínguez-Vega, J. Lancis, J.A. Monsoriu, Opt. Lett. 32 (2007) 853.
[18] B. Richards, E. Wolf, Proc. R. Soc. London Ser. A 253 (1959) 358.
[19] M. Gu, Advanced Optical Imaging Theory, Springer, Heidelberg, 2000.
[20] C.J. Zapata-Rodríguez, M.T. Caballero, Opt. Lett. 32 (2007) 2472.
[21] A. Pe'er, D. Wang, A. Lohmann, A.A. Friesem, Opt. Lett. 25 (2000) 776.